CHEMICAL ENGINEERING TRANSACTIONS
VOL. 35, 2013
A publication of AIDIC
The Italian Association of Chemical Engineering
www.aidic.it/cet
Guest Editors: Petar Varbanov, Jiří Klemeš, Panos Seferlis, Athanasios I. Papadopoulos, Spyros Voutetakis

ISBN 978-88-95608-26-6; **ISSN** 1974-9791
DOI: 10.3303/CET1335159

Analysis and Implementation of a Plant-Wide Control System for an LPG Reforming-Fuel Cell Power System

Dimitris Ipsakis[a], Simira Papadopoulou[a,b], Spyros Voutetakis[a,*], Panos Seferlis[a,c]

[a]Chemical Process & Energy Resources Institute (C.P.E.R.I.), Centre for Research and Technology Hellas (CE.R.T.H.), P.O. Box 60361, 57001, Thermi-Thessaloniki, Greece
[b]Automation Department, Alexander Technological Educational Institute of Thessaloniki, P.O. Box 141, 57400 Thessaloniki, Greece
[c]Department of Mechanical Engineering, Aristotle University of Thessaloniki, P.O. Box 484, 54124 Thessaloniki, Greece
paris@cperi.certh.gr

The core aim of this study is the development of a plant-wide control system for a pilot plant scale power unit based on LPG fuel processing. The system consists of the LPG steam reformer for the production of hydrogen followed by a water-gas-shift reactor, both of fixed-bed geometry. A polymer electrolyte membrane (PEM) fuel cell utilizes the reformer's hydrogen and enables power generation and delivery to a lithium-ion (Li-Ion) accumulator, thus simulating in this way a compact vehicular-oriented application. Heat integration in the system is achieved through a heat exchanger network mainly consisted of a burner that exploits the anode unconverted hydrogen and uses an individual LPG feed and a series of air coolers that enable efficient system autonomy. The main control objectives are the minimization of the system start-up time, the elimination of temperature overshoots in the reforming and water-gas-shift reactors as well as the effective alleviation of process disturbances during operation (mainly due to reaction thermal imbalances and catalyst deactivation). A multi-loop digital plant-wide control scheme utilizing PID controllers is proposed and tuned for optimal control error under several dynamic scenarios associated with the control objectives. Dynamic performance assessment of the control scheme is achieved through simulated cases utilizing a dynamic non-linear mathematical model for the integrated system. The proposed control scheme performed successfully under reference trajectory tracking and disturbance rejection scenarios.

1. Introduction

Hydrogen exploitation is under the footlight of numerous applications ranging from feedstock supply in petrochemical industry, in transportation sector and as an energy carrier in providing electricity to stand-alone applications. Such applications are indicated as a prerequisite for the on-board production from hydrogen containing fuels, where the most reliable and quite mature technology is steam reforming. Smith et al (2012) proposed a thermally integrated system, whereas Northrop et al., (2012) presented a fully automated system. Besides the development of a dynamic mathematical model, which is an essential requirement of simulated studies and has been presented in the past (Arpornwichanop et al., 2011), analysis and design of suitable control systems, imposes an indispensable research area that complements the overall operation of integrated power systems. Lin et al. (2006) developed dynamic reduced-order models for a methane reforming unit and utilized them in the performance evaluation of a conventional PID control scheme. Similarly, Hu et al. (2008) used linearized models in a feed-forward control scheme in a gasoline reforming unit. Both studies highlighted the need for the development of highly efficient control systems that can cope with the highly interactive nature of fuel processing and power generation systems. On the other hand, an advanced decentralized control framework for a reforming-fuel cell system was presented by Pukrushpan et al. (2006) that however analyzed the chemical process subsystems in a limited way. Generally, in all previous studies a systematic investigation of the

Please cite this article as: Ipsakis D., Papadopoulou S., Voutetakis S., Seferlis P., 2013, Analysis and implementation of a plant-wide control system for an lpg reforming-fuel cell power system, Chemical Engineering Transactions, 35, 955-960 DOI:10.3303/CET1335159

control performance under the variety of conditions that such systems operate is missing. Most research studies on hydrocarbons reforming focus on the development of rather case-oriented control schemes, without delving into details such as controller tuning, suitable pairing of variables and the achievement of the overall control objectives. In addition, nearly all studies consider only the fuel processor and rarely combine it with the power generation and the energy accumulation systems. The main objective of this work is the development of an efficient control system for an integrated fuel reformer-fuel cell system that will continuously provide electric energy to a Li-Ion accumulator at the desired rate. Simultaneously, the control system is responsible for ensuring the maintenance of reaction temperature levels within safety limits despite expected dynamic transients (e.g., promotion of undesired reactions, low heat transfer rates and so forth). The control scheme relies on suitable selection of controlled and manipulated variables, appropriate variables pairing, and the incorporation of efficient control algorithms.

2. Process flowsheet description

Figure 1 shows the schematic flow diagram of the LPG steam reforming-fuel cell power system that provides electric energy to a Li-Ion accumulator. Clearly, the end-user could be a vehicular application such as a forklift. At the feeding section, water is evaporated in heat exchanger E1 with the use of the hot effluent burner stream. The gas feed mixture water and LPG (mixer) is further heated in E2 by the reformer outlet before entering the plug flow reactor for hydrogen production. The reformer outlet stream after an initial cooling in E2, is subsequently air-cooled in E3 and then enters the high temperature shift reactor (HTS) for CO minimization to a level less than 1,000 ppm due to the constraint set by the PEM fuel cell operation. Since a significant amount of water is contained at the HTS outlet, a condenser is installed for water removal. The hydrogen rich stream with a content of approximately 75 % in hydrogen is then heated in unit E4 prior to its entrance in the high temperature PEM fuel cell anode. Power generation takes place in the fuel cell and electric energy is then directed to the Li-Ion battery. The anode effluent stream that contains the unreacted hydrogen along with fresh LPG are mixed as the main fuels in the burner.

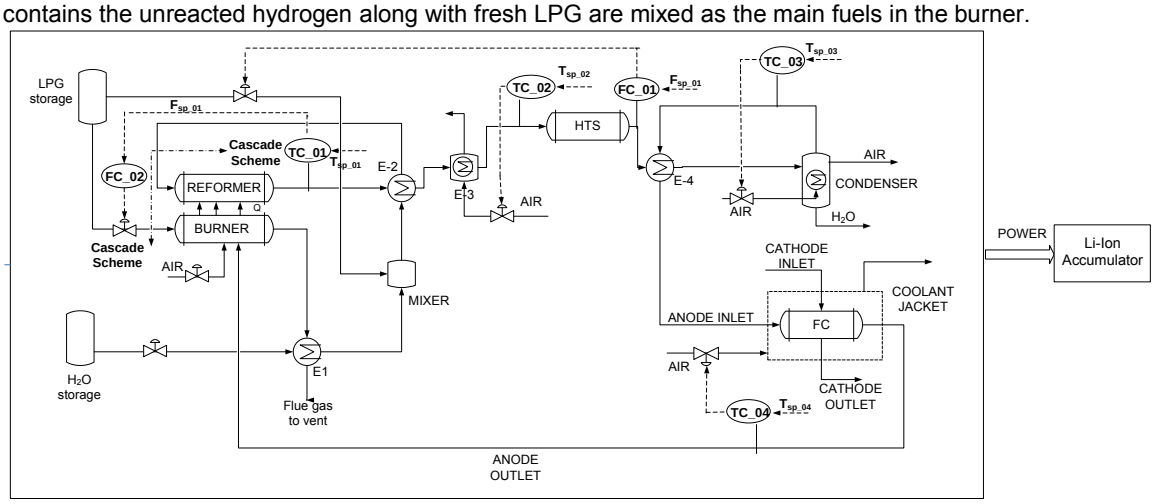

Figure 1: LPG reforming and fuel cell power system

Table 1: Reaction scheme of the LPG reforming and fuel cell power system

Subsystem	Reaction	Subsystem	Reaction
Reformer	$C_3H_8 + 3{\cdot}H_2O \rightarrow 3{\cdot}CO + 7{\cdot}H_2$	**Burner**	$C_3H_8 + 5O_2 \rightarrow 3CO_2 + 4H_2O$
	$C_4H_{10} + 4{\cdot}H_2O \rightarrow 4{\cdot}CO + 9{\cdot}H_2$		$C_4H_{10} + 6.5O_2 \rightarrow 4CO_2 + 5H_2O$
	$CO + H_2O \leftrightarrow H_2 + CO_2$,		$CH_4 + 2O_2 \rightarrow CO_2 + 2H_2O$
	$CO + 3{\cdot}H_2 \rightarrow CH_4 + H_2O$		$CO + 0.5O_2 \rightarrow CO_2$
			$H_2 + 0.5O_2 \rightarrow H_2O$
Water Gas Shift	$CO + H_2O \leftrightarrow H_2 + CO_2$	**Fuel Cell**	$H_2 + 0.5O_2 \rightarrow H_2O$

Table 1 presents the overall reaction scheme for the four main subsystems. The kinetic expressions follow an Arrhenius expression assuming pseudo-homogeneous reactions:

$$r_j = W_{cat} k_{j,o} \cdot \exp\left(-\frac{E_J}{RT}\right) \cdot \prod C_i^{a_i} \qquad (1)$$

where r_j is the reaction rate in mol/m^3·s, W_{cat} is the catalyst weight in kg, E_j and $k_{j,o}$ are the kinetic parameters, R is the ideal gas constant in J/mol·K, T is the reaction temperature in K, α_i is the reaction order and C_i is the component (reactant) concentration in mol/m^3

3. Control Objectives and Design of the Decentralized Control Scheme

The integrated fuel processor-fuel cell system must satisfy the following control objectives: a) Ensure fast response during start-up (<500 s), b) satisfy the defined power specifications, c) eliminate overshoot in the reactor temperatures during power level transition (maximum peak response lower than 10 K), d) alleviate quickly and efficiently the effects of disturbances on the control objectives. As controlled variables are selected those variables that are closely related to the control objectives. Reformer temperature, HTS inlet temperature, and HTS hydrogen concentration guarantee the desired fuel conversion to hydrogen and the satisfaction of the CO level in the fuel cell stream. Fuel cell inlet temperature and fuel cell operating temperature enable an efficient fuel cell operation and the satisfaction of the power level specification. LPG feed flowrate in the reformer is used for the control of hydrogen content in the product stream, whereas LPG feed flowrate in the burner maintains the crucial heat balance at the reformer and subsequently the entire system. The heat transfer at the E3 and the condenser are regulated by the air flow. A cascade control scheme is used to improve the regulation of the heat balance in the reformer and enhance the performance of the control system. The master loop the regulates the reformer outlet temperature with the LPG burner feed stream provides the setpoint for the much faster secondary control loop that uses the burner temperature as an indication of disturbances in the burner. Obviously, the heat balance in the reformer is of paramount importance for the hydrogen production and eventually the power generation. Table 2 shows the pairing of all controlled and manipulated variables in the individual control loops.

Table 2: System Controlled and manipulated variables

Controlled Variables	Manipulated Variables	Controller Indication
Reformer outlet temperature	Setpoint for LPG flowrate at burner	TC_01
Burner temperature	LPG flowrate at burner	FC_02
HTS inlet temperature	Air flowate at E3	TC_02
Fuel cell inlet temperature	Air flow rate at condenser	TC_03
Fuel cell operating temperature	Water flowrate at cooling jacket	TC_04
HTS hydrogen concentration	LPG flowrate at reformer	FC_01

4. Mathematical modeling

The non-linear dynamic model for the fuel processors and heat exchanging subunits consists of: a) component molar balances, b) energy balances, and c) constitutive equations that complement the balance equations. The assumptions that accompany the mathematical model are: a) ideal gas behavior, b) insignificant spatial variation, c) negligible system pressure drop and e) pseudo-homogeneous kinetics. Eq(2) and Eq(3) provide the molar and energy balances respectively:

$$\frac{dn_i}{dt} = \frac{d(C_{i,out}V)}{dt} = C_{i,in}Q_{in} - C_{i,out}Q_{out} \pm \sum v_{i,j} r_{i,j} \tag{2}$$

$$\frac{d(\rho_{out} c_p V T_{out})}{dt} = c_p(\rho_{in}Q_{in}T_{in} - \rho_{out}Q_{out}T_{out}) \pm \sum Q_{th} \tag{3}$$

Symbol n_i denotes the i-th component moles in mol, V the mixture volume in m^3, Q the volumetric flowrate in m^3/s, $r_{i,j}$ the j-th reaction rate of the i-th component in mol/m^3·s, $v_{i,j}$ the stoichiometric coefficient of i-th component in the j-th reaction, T_{out} the outlet stream temperature in K, c_p the specific heat capacity in J/K·kg, ρ_{out} the mixture total density in kg/m^3, and ΣQ_{th} the sum of the total heat exchange (e.g., heat losses to surroundings, heat due to electrochemical reactions, heat reaction or stream exchange in W).
In the case of reformer-burner coupling an additional set of equations is needed in order to derive the dynamics of the wall temperature interaction.

$$(mc_p)_{burner}\frac{dT_{burner,wall}}{dt} = UA_{burner,in}(T_{burner,out} - T_{burner,wall}) - UA_{reformer,wall}(T_{burner,wall} - T_{reformer,wall}) \tag{4}$$

$$(mc_p)_{reformer}\frac{dT_{reformer,wall}}{dt}=UA_{reformer,wall}(T_{burner,wall}-T_{reformer,wall})-UA_{reformer,in}(T_{reformer,wall}-T_{reformer,out}) \quad (5)$$

Symbol m denotes the subsystem mass in kg, c_p the subsystem specific heat capacity in J/K·kg, $T_{burner,wall}$ and $T_{reformer,wall}$ the subsystem wall temperature in K, $T_{burner,out}$ and $T_{reformer,out}$ the fluid outlet temperature in K, $UA_{burner,in}$ and $UA_{reformer,in}$ the overall heat transfer coefficient from bulk to wall in W/K, and $UA_{burner,wall}$ and $UA_{reformer,wall}$ the overall heat transfer coefficient from wall to wall in W/K. The volumetric flowrate, concentration and molar flowrate are given by:

$$Q_{in/out}=\frac{\sum_{i=1}^{N}F_{i,in/out}RT_{in/out}}{P} \quad \text{and} \quad C_{i,in/out}=\frac{F_{i,in/out}}{Q_{in/out}} \quad (6)$$

Subscripts *in/out* denote the inlet/outlet of a subsystem and F_i the i-th component flowrate in mol/s. In the case of the fuel cell, there is a linear dependence of current draw and hydrogen consumption via the Faraday's law, whereas the fuel cell operating voltage (V_{fc}, *Volt*) is based on a group of non-linear equations (Ipsakis et al., 2012a) that is dependent on various system variables such as temperature (T_{fc}, *K*), component concentrations ($C_{i,fc}$, *mol/m*^{3}), operating current (I_{fc}, *A*), design characteristics (d), and electrochemical parameters (p):

$$R_{fc}=\frac{n_c\cdot I_{fc}}{n_e\cdot F}\cdot n_f \quad \text{and} \quad V_{fc}=f(T_{fc},C_{i,fc},I_{fc},d,p) \quad (7)$$

Symbol R_{fc} denotes the reaction rate in mol/s, n_c are the number of cells, I_{fc} the operation current in A, n_e the number of electrons, F the Faraday's constant in Cb/mol, and n_f is the fuel cell electrical efficiency.
The Li-Ion accumulator modeling involves the voltage-current relationship that has been adapted from a non-linear model (Manwell and McGowan, 1993) where it is assumed for the current stage that operating temperature is constant. Accumulator voltage is dependent on lumped parameters (E_{ac},*Volt*), capacity (Q_{ac}, *Ah*), current (I_{ac},*A*), and resistance (R_o, *Ω*) shown below.

$$V_{ac}=f(E_{ac},Q_{ac},I_{ac},R_o) \quad (8)$$

The state-of-charge (SOC) of the accumulator is provided by Eq. 9 and simply states the available fraction of power at each time instance:

$$SOC(t+1)=SOC(t)\cdot(1-\sigma_{ac})+\frac{I_{ac}\cdot\eta_{ac}}{Q_{ac}}\cdot(\Delta t) \quad (9)$$

Symbol η_{ac} denotes the accumulator efficiency (~95 %), σ_{ac} the self-discharge rate (~2.5 %), and Δt the time difference (t+1)-(t) in h.

5. Control System Performance

5.1 Controller Tuning and Optimal Selection

Discrete proportional-integral-derivative (PID) controllers in their velocity form have been implemented in every control loop described at Table 2. Controller tuning parameters have been calculated through the optimization of the integral of squared errors, $\varepsilon(t)$, for all controlled variables. Initial values for the controller parameters have been provided by the Ziegler-Nichols method (Bequette, 2003).

$$\begin{aligned}&\underset{c}{Min}\quad J=\int_0^{\infty}\varepsilon^2(t)dt\\&s.t.\quad \frac{dx}{dt}=h(x,u,c)=0,\\&u^l\le u\le u^u,\ x^l\le x\le x^u,\ c^l\le c\le c^u\end{aligned} \quad (10)$$

Symbol $c(t)$ denotes the set of controller parameters; namely the proportional gain, K_c , the integral time, τ_I, and the derivative time, τ_d, $x(t)$ the state variables, $u(t)$ the manipulated variables, and $\varepsilon(t)$ the time varying error for the controlled variables in each control loop. Symbol h denotes the differential equations of the system provided from the mathematical model. Table 3 provides the optimal values for the control parameters as obtained from the solution of the optimization problem.

Table 3: Finely Tuned PID controller parameters (5s sampling time)

Controller Indication	Controller Parameters	Controller Type
TC_01 / FC_02	K_c=2.310^{-4} /2.310^{-5}, τ_I=150 s / 30 s, τ_d=7 s / 2 s	PID
TC_02	K_c=5.910^{-1}, τ_I=130 s, τ_d =10 s	PID
TC_03	K_c=2.910^{-1}, τ_I=150 s, τ_d =13.75 s	PID
TC_04	K_c=4.710^{-4}, τ_I=100 s, τ_d= 15.75 s	PID
FC_01	K_c=4, τ_I=100 s, τ_d=4.32 s	PID

5.2 Evaluation of Controller Performance

The performance of the proposed control system is evaluated in a number of simulated scenarios. In the first case, the performance of the system in start-up conditions followed by a 20 % increase in power requirements (practically at hydrogen flowrate) at *t*=2000 s. In the second case, the performance of the controllers to an unmeasured disturbance is investigated. Specifically, at *t*=2000 s the catalyst activity is reduced by 20 %. The overall results are presented in Figs. 2a-d.

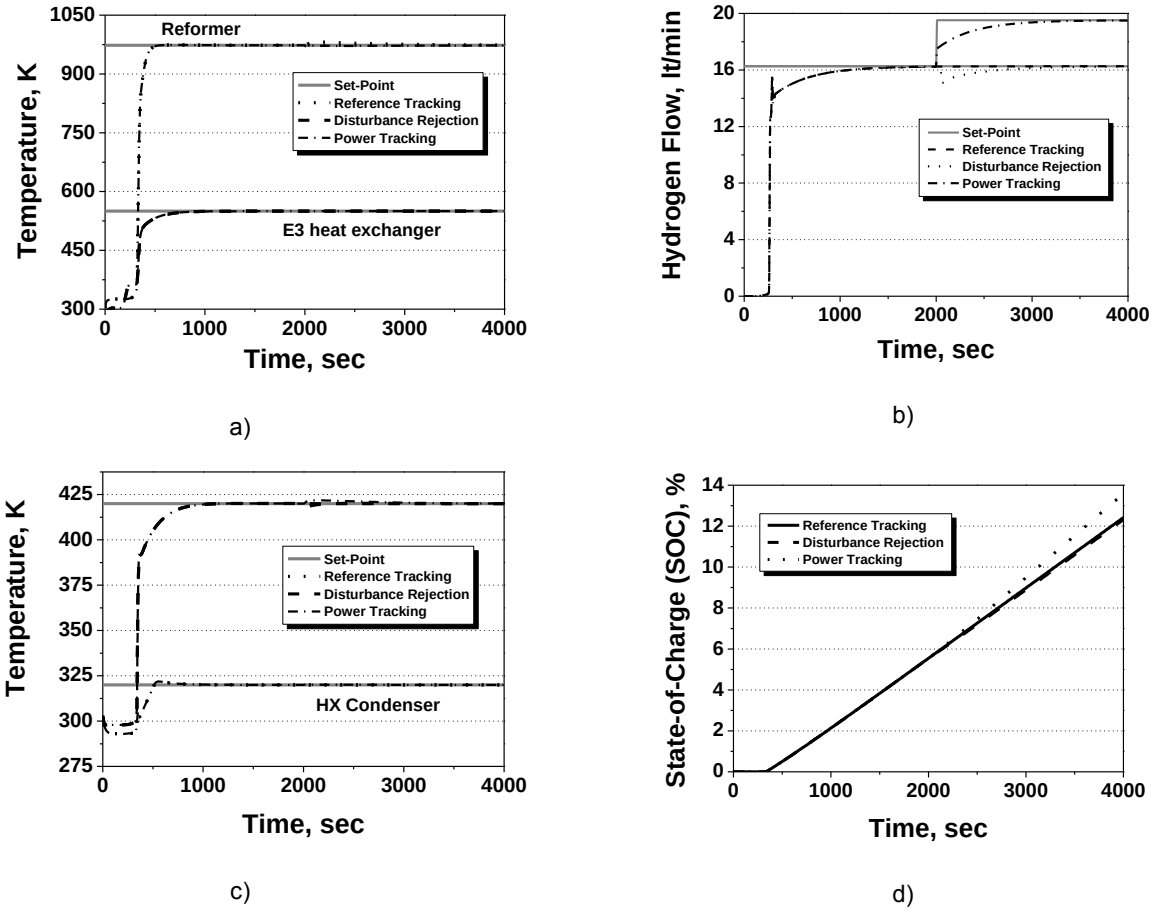

Figure 2: a) Reformer exit and HTS inlet temperature, b) hydrogen flow at Fuel Cell anode, c) fuel cell operating and HX condenser exit temperature and d) accumulator state-of-charge

During reference tracking, controlled variables exhibit zero steady-state error and minimal overshoot. The start-up time of the integrated unit is quite satisfactory and around the desired level of 500 s. The disturbance of the catalyst activity causes an increase at the reformer temperature (inverse promotion of endothermic reactions), that is quickly compensated by the cascade controller. The other temperature controllers are not affected significantly by this disturbance. However, hydrogen flowrate at HTS exit is affected more by the disturbance, since reduction in catalyst activity reduces hydrogen production, and the transition up to reference case takes around 650 s. This slow response is normal (nearly equal to start-up times) considering that many subsystems are involved between the HTS effluent stream and the LPG feed

stream at the reformer. Power reference tracking through the implementation of suitable setpoints for the HTS hydrogen flowrate is achieved. Due to higher hydrogen at the anode, fuel cell temperature is increased at t=2000 s, but quickly returned to referenced state. A very small deviation occurs at the reformer temperature, but with no significant problems. The decrease in the hydrogen production at the disturbance case and the increase in the hydrogen production during the power tracking case, cause changes in the accumulator charging procedure. At both simulated scenarios, the accumulator was initialized as totally empty, meaning at t = 0 the SOC was 0 %, while at t = 4,000 s the SOC was 12.42 % in the reference tracking case, 12.32 % in the disturbance rejection scenario and 13.6 % in the power tracking scenario.

6. Conclusions

A highly performing control scheme has been properly designed for an integrated LPG reforming-fuel cell-accumulator system. First, a suitable selection of controlled and manipulated variables according to the control objectives has been selected and paired using the knowledge about the dynamic behavior of the system. Multi-loop PID controllers were implemented to the system and optimally tuned for optimal performance. A set of simulated scenarios covering both reference tracking and disturbance rejection cases demonstrated the ability of the control system to satisfy the control objectives.

Acknowledgment

This study is conducted under the National Research Projects Framework and Co-financed by National Strategic Reference Framework (NSRF) 2007-2013 of Greece and the European Union – program “Cooperation 2009-ACT-I” (09-ΣΥΝ-51-453).

References

Arpornwichanop A., Wasuleewan M., Patcharavorachot Y., Assabumrungrat S., 2011, Investigation of a dual-bed autothermal reforming of methane for hydrogen production, Chemical Engineering Transactions, 25, 929-934, DOI: 10.3303/CET1125155.

Bequette B.W., 2003. Process Control: Modeling, Design and Simulation, Prentice Hall, New Jersey, USA.

Hu Y., Chmielewski D.J., Papadias D., 2008. Autothermal reforming of gasoline for fuel cell applications: Controller design and analysis, Journal of Power Sources, 182, 298-306.

Ipsakis D., Voutetakis S., Papadopoulou S., Seferlis P., 2012a. Optimal operability by design in a methanol reforming-PEM fuel cell autonomous power system, International Journal of Hydrogen Energy, 37, 16697-16710.

Ipsakis D., Voutetakis S., Papadopoulou S., Seferlis P., Elmasides C., Papadaki K., Mastrogeorgopoulos S., Kyriakides A., 2012b. Dynamic modeling and control of a steam reformer-fuel cell power system operating on LPG for vehicular applications, Chemical Engineering Transactions, 29, 49-54, DOI: 10.3303/CET1229009.

Lin S. T., Chen Y.H., Yu C.C., Liu Y.C., Lee C.H., 2006. Dynamic modeling and control structure design of an experimental fuel processor, International Journal of Hydrogen Energy, 31, 413-426.

Manwell J.F., McGowan J.G., 1993. Lead acid battery storage model for hybrid energy systems, Solar Energy, 50, 399–405.

Northrop W.F., Choi S.O., Thompson L.T., 2012. Thermally integrated fuel processor design for fuel cell applications, International Journal of Hydrogen Energy, 37, 3447-3458.

Pukrushpan J., Stefanopoulou A., Varigonda S., Eborn J., Haugstetter C., 2006. Control-oriented model of fuel processor for hydrogen generation in fuel cell applications, Control Engineering Practice, 14, 277-293.

Smith R., Zhang N., Zhao J. 2012. Hydrogen integration in petroleum refining, Chemical Engineering Transactions, 29, 1099-1104, DOI: 10.3303/CET1229184.